Journal of Materials Chemistry B

Accepted Manuscript

ROYAL SOCIETY OF CHEMISTRY

www.rsc.org/materialsB

Titania as driving agent for DHICA polymerization: a novel strategy for the design of bioinspired antimicrobial nanomaterials

Giuseppe Vitiello,[a,b] Alessandro Pezzella,[c] Anna Zanfardino,[d] Mario Varcamonti,[d] Brigida Silvestri,[a] Aniello Costantini,[a] Francesco Branda[a] and Giuseppina Luciani[a,*]

[a] Dipartimento di Ingegneria Chimica, dei Materiali e della Produzione Industriale, Università di Napoli "Federico II", p.le V. Tecchio 80, 80125Napoli, Italy.

[b] CSGI, Consorzio Interuniversitario per lo Sviluppo dei Sistemi a Grande Interfase, Italy.

[c] Dipartimento di Scienze Chimiche, Università di Napoli "Federico II" via Cintia 4, 80126 Napoli, Italy.

[d] Dipartimento di Biologia, Università di Napoli "Federico II" via Cintia 4, 80126Napoli, Italy.

* Corresponding author. Tel.:+390817682433; Fax: +390817682595.

E-mail address: giuseppina.luciani@unina.it

Abstract

Organic materials are widely employed to tune surface chemistry and/or as structuring agent of inorganic materials. Here, we propose a novel synthetic approach whereby TiO_2 not only promotes 5,6-dihydroxyindole-2-carboxylic acid (DHICA) polymerization but also acts as templating agent for the forming eumelanin itself. Hybrid TiO_2-DHICAmelanin nanostructures have been produced, showing biocide activity even under visible light condition (activation). Hybrid nanostructures have been analyzed and characterized by multiple techniques, proving that both organic and inorganic phases strongly affect each other during *in-situ* formation, as far as it concerns both morphology and microstructure, conferring unique biocide properties to the resulting nanomaterials. This strategy ensures much more far-reaching implementation in the synthesis of hybrid nanosystems, opening new perspectives in the design of multifunctional materials.

Keywords: nanomaterials, TiO_2, DHICA, eumelanin, radicals, antimicrobial

Introduction

An increasing interest has been recently growing on organic-inorganic hybrids as creative alternative for obtaining new multifunctional nanomaterials. These hybrids made by coupling organic molecules to inorganic nanostructures, not only combine the often dissimilar properties of inorganic and organic components in one material, but also actually provide the opportunity to invent a huge set of new multifunctional materials with a large spectrum of known and as yet unknown properties.[1] A large number of recent literature data actually focus on modification/modulation of surface chemistry of inorganic materials in order to improve their functional properties.[2,3] Alternatively, organic components play a key role in structuring the inorganic phase.[3]

Herein, we provide a novel synthetic approach whereby inorganic materials are employed as active and templating agents for formation of organic polymers. This bioinspired synthetic strategy has been exploited to produce eco-friendly hybrid nanostructures with antimicrobial activity even under visible light induction condition, following a bioinspired approach.

Eumelanins are negatively charged, hydrophobic pigments of high molecular weight, widely dispersed in mammalians, plants and microorganisms.[4,5] Many studies have recently shown that melanins interfere with numerous host defense mechanisms: they are highly immunogenic[6] and have anti-inflammatory properties[7], protecting organisms against UV-radiation[8-15] as well as microbial lysis.[16,17] Indeed, melanization of skin and other tissues is an important component of the innate immune defense system: in this, the function of eumelanin in skin seems to inhibit the proliferation of bacterial, fungal and other parasitic infections of the dermis and epidermis.[18,19] In particular, eumelanins[20] are produced by oxidation of tyrosine through tyrosinase to DOPA (o-dihydroxyphenylalanine) and dopachrome, further the cyclization mediates to form 5,6-dihydroxyindole (DHI) or 5,6-dihydroxyindole-2-carboxylic acid (DHICA).[4] Since isolation of natural eumelanins is a very difficult task, it is possible to mimic their formation by oxidizing in

vitro DHI[20] and DHICA[21] obtaining synthetic eumelanin models quite similar to the natural pigment.[4,20]

Titanium dioxide (TiO_2, titania) is an inexpensive, environmentally friendly, nontoxic and photostable material, as well as high performance catalyst in photo-oxidative processes.[22,23]

In this paper, this TiO_2 property has been actually exploited to catalyze DHICA polymerization through oxidative reactions. In details, TiO_2-DHICAmelanin hybrids were prepared through *in-situ* methodology based on hydrothermal route. Morphology of nanostructures was investigated through transmission electron microscopy (TEM). The specific surface area and pore size distribution were also evaluated by BET porosimetry. Influence of DHICA-melanin on crystal structure of TiO_2 was assessed by X-ray diffraction (XRD). Furthermore, electron paramagnetic resonance (EPR) spectroscopy provided information about the presence of intrinsic radical species and their distribution within the nanostructures. Optical properties of these materials were also evaluated through Diffuse Reflectance UV-VIS (DRUV) spectroscopy. Finally, tests on bacterial pathogens in the absence and presence of UV-irradiation proved antimicrobial activity of these nanomaterials even under visible light. By in-depth overview, we linked antimicrobial activity to the physico-chemical properties of these nanosystems.

This research is inspired by the growing interest on hybrid titania-based materials. Most of studies reported in literature are focused on narrowing the band gap of TiO_2 in order to have photocatalytic behavior even under visible light, as well as avoiding fast recombination of charge carriers (e^-/h^+) in order to improve photo catalytic performance.[24] To the best of our knowledge, this study sets up a novel role for TiO_2 which acts as both catalyst and structuring direct agent for the growing polymeric/organic phase.

In this scenario, the proposed methodology defines a new potential synthetic strategy for the design and production of hybrid nanomaterials. In addition, the proposed hybrid systems have intrinsic potent antimicrobial activity even under environmental light. Biocide properties as well as non-toxic and bio-friendly nature of both organic and inorganic components make these materials very

intriguing as a synthetic platform to produce antimicrobial formulations for biomedical and food packaging applications.

Experimental Section

Materials

Titanium isopropoxide (TTiP), isopropanol, acetic acid, and triethylamine (TEA) were purchased from Sigma Aldrich and used as received. DHICA monomer was prepared as described elsewhere.[25]

Synthesis of TiO_2 nanoparticles

TiO_2 nanoparticles were prepared by hydrothermal synthesis.[26,27] A typical precursor solution was obtained by adding dropwise 6 mL of Tiisopropoxide (TTiP)/isopropanol solution (Sol-1, 3.38 M in TTiP) to 31.3 mL of water solution at pH 1.5 achieved by means of acetic acid (Sol-2). After Sol-1 addition a white precipitate was obtained that upon stirring at room temperature for two days led to a yellowish colloidal solution, thus indicating resuspension of the precipitate and reduction of the particles size below 20 nm.[28] Triethylamine (TEA) was then added dropwise to the TiO_2 colloidal solution till pH=7. The obtained white precipitate suspension was then sealed within a Teflon recipient (the liquid volume corresponding to 75% of the whole), placed into a circulating oven and kept at 120 °C for 24 h. TiO_2 powders were obtained by centrifugation and repeated washing (3 times with distilled water). Then, obtained precipitates were re-suspended water.

Synthesis of hybrid DHICA-TiO_2 nanoparticles

Hybrid TiO_2-DHICA nanoparticles were prepared *in situ* following almost the same procedure as bare nanoparticles. Briefly, Sol-1(6 mL) was added drop-wise to Sol-2 (31.3 mL) and the mixture was kept stirred for two days leading to TiO_2 colloidal solution. Then, 10 mg of DHICA for 1.193 mL of TTiP were added just before neutralization with TEA till pH 7. Solution turned brown just after DHICA addition. This sample will be named in the following as TiO_2-DHICA_ti. Finally, the obtained suspension was sealed within a Teflon recipient (the liquid volume corresponding to 75% of the whole), placed into a circulating oven and kept at 120 °C for 24h.[27]

TiO_2-DHICA_ti nanoparticles recovered after hydrothermal treatment were submitted to oxidation by exposure to an oxidizing atmosphere (e.g. oxygen atmosphere and ammonia vapors).[29] In the general procedure, the appropriate suspension (hybrid nanoparticles or DHICA) was incubated in the oxygen/ammonia atmosphere at controlled temperature (25-40 °C). The ammonia vapors were produced by equilibration of the atmosphere with ammonia solution (28% to 7% NH_3 in H_2O) in a sealed camera at 1atm pressure. Exposure times varied in the range 2 to 18 h. These samples will be named as TiO_2-DHICA_polym in the following. Bare DHICA-melanin nanoparticles, as a reference, were also prepared using the same procedure.

Physico-chemical characterization

In order to perform oxidative degradation[30] of hybrid DHICA-titania nanoparticles, a suspension of the appropriate sample (10 mg) in 1M K_2CO_3 (3 mL of water solution) was treated with 30% v/v H_2O_2 (20 μL of water solution) and vigorously stirred at 25 °C for 3 h. The reaction was stopped by addition of 5% w/w $NaHSO_3$ (500 μL). The mixture was acidified to around pH=2 with 1M HCl and extracted with ethyl acetate (4×1 mL). The combined organic layers were dried over sodium sulfate and evaporated to dryness. The residue was taken up in water (1 mL) and analyzed by HPLC using as the mobile phase a mixture of 0.05M citric acid and 0.3M formic acid containing 3% v/v acetonitrile brought to pH=2.5 with conc. ammonium hydroxide.

Morphological analysis of the prepared nanoparticles was carried out by Thermal Electron Microscopy (TEM). Samples for TEM were prepared by dispersing the obtained powders in aqueous solution and then placing a drop of suspension on one side of the transparent polymer coated 200 mesh copper grid. Samples were successively coated by carbon to increase the thermal and the electric conductivities of powders. TEM images have been taken with a PHILIPS EM208S microscope equipped with a Mega View camera for digital acquisition of images.

Crystalline phases of the titania-based nanosystems were identified by X-ray diffraction (XRD) experiments performed by using a PANalytical diffractometer with a nickel filter and Cu Kα radiation.

The specific surface area (S_{BET}) and the pore volume (V_P) of hybrid nanosytems were evaluated by generating seven-point isotherms at 77 K for N_2 adsorption (Autosorb-1, Quantachrome) using an amount of char sample capable to provide a specific surface area equal to 5 m^2 in the sample cell. The mesopore volume (V_{BJH}), the average pore radius (r_P) and the pore size distributions were estimated by the Barreto-Joyner-Halenda (BJH) method applied to the desorption branch of the isotherm.[31]

Electron Paramagnetic Resonance (EPR) spectroscopy experiments were carried out by means of X-band (9 GHz) Bruker Elexys E-500 spectrometer (Bruker, Rheinstetten, Germany), equipped with a super-high sensitivity probe head. Solid samples were transferred to flame-sealed glass capillaries which, in turn, were coaxially inserted in a standard 4 mm quartz sample tube. Measurements were performed at room temperature. The instrumental settings were as follows: sweep width, 100 G; resolution, 1024 points; modulation frequency, 100 kHz; modulation amplitude, 1.0 G. The amplitude of the field modulation was preventively checked to be low enough to avoid detectable signal overmodulation. Preliminarily, EPR spectra were measured with a microwave power of ~0.6mW to avoid microwave saturation of resonance absorption curve. Several scans, typically 32, were accumulated to improve the signal-to-noise ratio. Successively, for power saturation experiments, the microwave power was gradually incremented from 0.02 to 160 mW. The *g*-factor value was evaluated by means an internal standard (Mg/MnO)[32] which was inserted in the quartz sample tube co-axially with the capillary containing the samples. Free radical concentration in the sample was estimated by using a specific amount of MnO sample as reference. The area under the EPR absorption curves was estimated by double integration of their first derivatives.

Diffuse Reflectance UV–VIS (DRUV) measurements have been performed by using a Jasco spectrophotometer and $BaSO_4$ as a reference in the 190–850 nm wavelenghts range.

Antimicrobial assay

A single colony of *Escherichia coli* DH5α strain was re-suspended in 5 mL of LB medium (Becton Dickinson) and over-night incubated at 37 °C. When the culture reached an OD_{600} of 1 unit, it was diluted 1:100 in 20 mM, pH 7.0 NaP buffer. Samples were prepared by adding 40 μL of bacterial cells and the different compounds to test at a final concentration of 200 μg/mL, 1 mL final volume was reached with 20 mM pH 7.0 NaP buffer. Negative controls were represented by cells incubated without any compound or with BSA at the same concentration of tested molecules; cells incubated with ampicillin (0.05 mg/mL) were used as positive control. Samples were incubated at 37 °C for 4 hours and dilutions (1:100 and 1:1000) of all the samples were placed on solid LB medium and incubated over-night at 37 °C. The following day the survived cells were estimated by colonies counting on each plate and compared with the controls. All compounds were tested in triplicate experiments, standard deviations were always <5% for each experiment. Finally, all samples, TiO_2, DHICA-melanin, TiO_2-DHICA_ti, TiO_2-DHICA_polym, were also UV irradiated for 1 minute at wavelength of 254 and 366 nm before their inoculation into bacterial cells.

Results and Discussion

Melanin content determination

In order to validate chemical composition of hybrid-titania nanoparticles, a classical analytical procedure for eumelanin characterization was pursued.[30] The procedure involves the use of alkaline hydrogen peroxide as the oxidizing agent to induce degradation of the eumelanin pigment into easy to detect and quantify pyrrolecarboxylic acids to obtain indirect estimation of eumelanin content (Table 1).

	hybrid TiO_2nanoparticles	DHICA-melanin
Yield (nmol/mg sample)[a] PTCA	10.0	28.5
Melanin content estimation	28 %	100 %

[a]Determined by HPLC, average of three experiments, S.D.b5%.

Table 1. Yields[a] of pyrrole acids by oxidative degradation of hybrid nanoparticles and DHICA-melanin.

Data obtained do confirm that the eumelanin pigment is formed within the hybrids. In order to confirm the key role played by TiO_2 in polymerization of DHICA, hydrothermal synthesis was also carried out without the addition of TTiP to the mixture, as a control experiment. No particles were recovered from solution after the hydrothermal treatment, as demonstrated by the EPR spectrum (see Figure ESI3) which does not show any signal.

A possible mechanism of titania driven melanin formation can be hypothesized. It is well known that TEA leads to the precipitation of TiO_2 amorphous gel from Ti^{4+} aqueous solutions.[27,33] TiO_2 nanoparticles can be sensitized to visible light through adsorption of organic molecules (dye-sensitizers) onto the semiconductor surface. In the case of high molecular weight molecules, upon photoexcitation, an electron is transferred from the HOMO of the adsorbed molecule to the conduction band of the semiconductor, either directly or indirectly, via the LUMO of the adsorbed molecule. Alternatively, for small organic molecules, such as catechol and dopamine, the modifier adsorption leads to the formation of an adsorbate-to-nanoparticle (ligand-to-metal) charge-transfer complex, which absorbs visible light, inducing a direct injection of an electron from the ligand to the oxide conduction band.[34-36] Electrons injected into the conduction band by charge transfer complexes, have molecular oxygen reduced to superoxide ion O_2^-, a very reactive species in oxidative processes, that may involve even oxidation of the organic ligand. Indeed, it is known that catechol adsorbed onto titania surfaces, polymerizes under visible light.[34] Similarly, DHICA can adsorb onto TiO_2 and act as a ligand for Ti^{4+} ions, through its catechol group. Consequently, the

formed charge transfer complex activates oxidative polymerization of DHICA even under visible light. Moreover it is well established that metal ions[37] can promote 5,6-dihydroxyindole aerobic oxidation and it is expected Ti does behave as its close metal elements.[38]

Rough comparison with a DHICA melanin sample allows to estimate the pigment content in hybrid particles in the range of 20% w/w for both TiO_2-DHICA_ti and TiO_2-DHICA_polym.

TEM analysis

Morphology of the bare TiO_2 and hybrid TiO_2-DHICAnanoparticleswas observed with TEM (Fig. 1). DHICA-melanin micrography is also reported for comparison (Fig.1B).

As shown in Fig. 1A, bare TiO_2 nanosystems show rod-like structures (3x12 nm in size), while DHICA-melanin presents a cubic shape, about 30 nm in size. In contrast, different morphologies can be observed for TiO_2-DHICA_ti and TiO_2-DHICA_polym samples with respect to TiO_2: *in situ* procedure led to brownish rounded shaped particles, about 10 nm in size, due to a DHICA involvement in the growth of hybrid nanoparticles.[26] DHICA can actually act as a complexing agent for Ti^{4+} ions, through its catechol group. Furthermore, DHICA molecules may preferentially absorb onto specific planes during the growth of the particles.[39]

TEM micrographs (Figs. 4C and 4D) clearly indicate that no differences are detectable for the two TiO_2-DHICA_ti and TiO_2-DHICA_polym systems, as far as it concerns shape and size, suggesting that morphology of nanomaterials is defined by the hydrothermal synthesis.

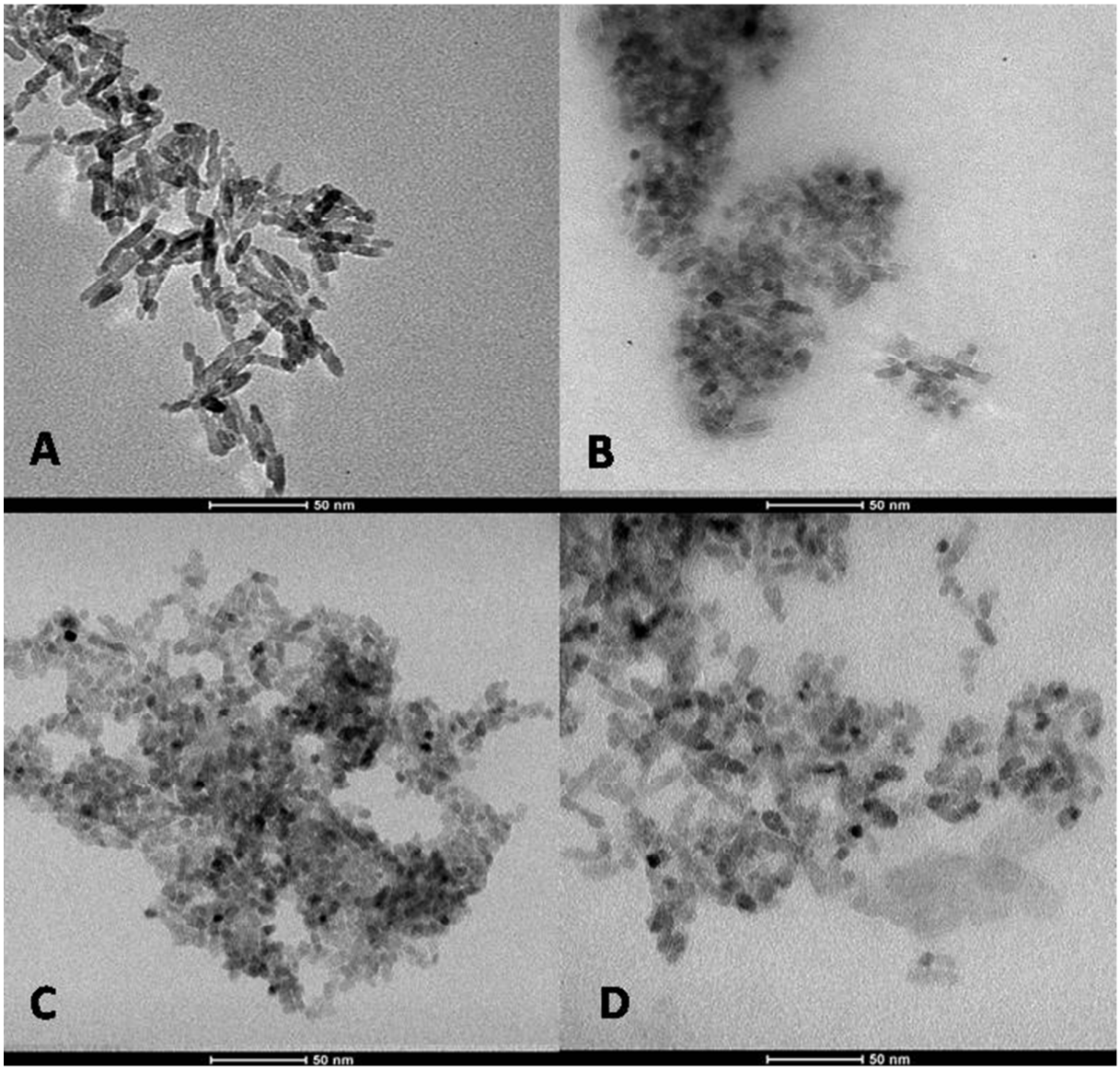

Fig. 1 TEM micrographs of bare TiO_2 (**A**), DHICA-melanin (**B**), TiO_2-DHICA_ti (**C**) and TiO_2-DHICA_polym (**D**) nanostructures.

XRD analysis

XRD patterns of the hybrid samples, reported in Electronic Supporting Information (Figure ESI1), are in agreement with the standard anatase profile (JCPDS 84–1286), both in terms of peak positions (i.e., the diffraction angles 2θ) and relative peak intensities[40] exhibiting strong diffraction peaks at 25° and 48°. Therefore, titania crystallized in the anatase structure in all samples.[41] Worth of note is that, the anatase pattern is featured also by TiO_2-DHICA_ti and TiO_2-DHICA_polym.

The latter shows sharper width at half height than both bare TiO_2 and TiO_2-DHICA_ti, suggesting larger dimensions of the crystals within the particles (about 4.0 nm determined by Sherrer formula).

Surface area and pore distribution

Nitrogen adsorption-desorption isotherms of bare TiO_2 and hybrid TiO_2-DHICA_melanin nanostructures are shown in Fig. 2A. All samples show a type-IV isotherm, with a type-H2 desorption hysteresis loop[42], typical of mesoporous solids. This is confirmed by pore size distribution curves (Fig. 2B), indicating that all systems have mesopores with size in the range 2-4 nm (Table 2). Furthermore, pore size distribution of TiO_2-DHICA_polym shows a pronounced shoulder at about 1.8 nm, suggesting the presence of micropores within the sample. Mesopores size is narrower in the TiO_2-melanin hybrids, suggesting that *in situ* formation of both melanin and titania during the hydrothermal process produces an intimate mixture of the organic and inorganic components. Moreover, the further polymerization step of DHICA after hydrothermal treatment (TiO_2-DHICA_polym) is supposed to produce high molecular weight oligomers within the pores, thus decreasing their size, and increasing the micropores, as shown in Fig. 2B. Finally, DHICA polymerization within the pores must partially seal porosity and lead to a decrease of specific surface area (see Table 2). As reference, the surface area of DHICA-melanin nanostructures is also determined, showing a very low value equal to 28.53 m²/g.

	TiO_2	**TiO_2-DHICA_ti**	**TiO_2-DHICA_polym**
Surface Area (m²/g)	190.3	191.4	171.7
Pore Volume (cc/g)	0.30	0.27	0.19
Pore Radius (Å)	37.1	31.4	23.7

Table 2. BET surface area and pore properties of the resulting hybrid nanoparticles.

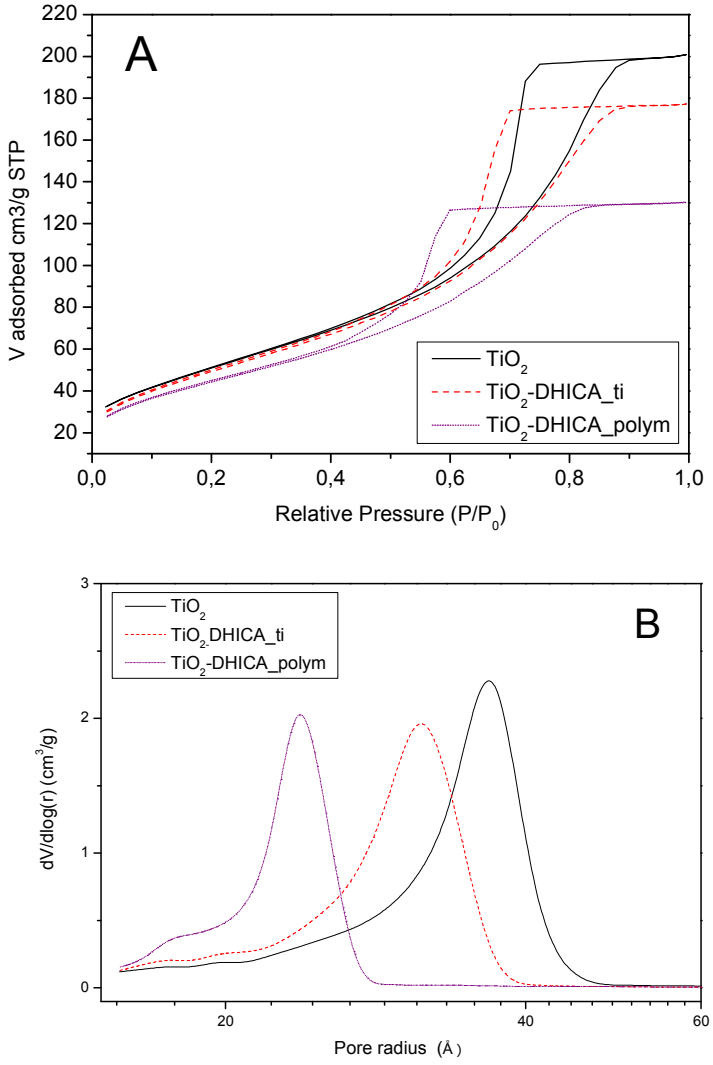

Fig. 2 Adsorption-desorption isotherms of nitrogen (**A**). BJH distribution curves for bare TiO_2 and hybrid melanin-based nanoparticles (**B**).

EPR analysis

EPR measurements on TiO_2 and DHICA-hybrid TiO_2nanosystems were performed by following an experimental procedure recently used in the characterization of melanins.[43,44] Analysis of this EPR signal provides significant information on the nature of the paramagnetic centers and on the supramolecular properties of solid materials. In this study, we undertook an EPR characterization of powdered samples synthesized as previously described. All EPR spectra are reported in Fig. 3,

whereas the spectral parameters calculated from them are summarized in Table 3. By observing Fig. 3A, no signal was detected for neat TiO_2 (spectrum A), indicating no oxygen vacancy or Ti^{3+}in these powder which is consistent with previous reports that indicates no EPR signal for pure TiO_2.[22,43] In Fig.3, the spectra B, C and D represent the spectra of TiO_2-DHICA_ti, TiO_2-DHICA_polym and DHICA-melanin, respectively.

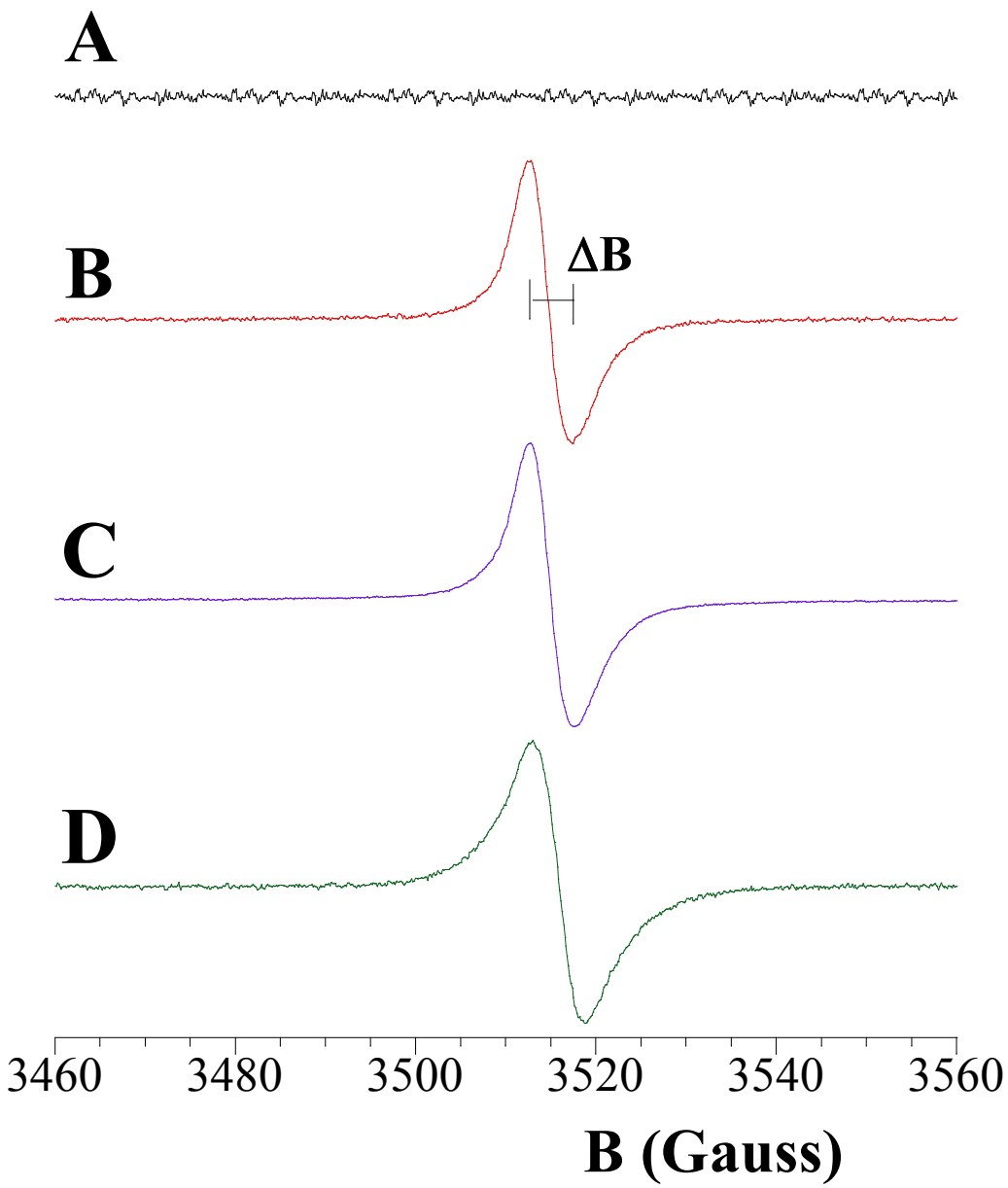

Fig.3 EPR spectra of TiO_2 (**A**), TiO_2-DHICA_ti (**B**) TiO_2-DHICA_polym (**C**) and DHICA-melanin (**D**) nanosystems.

They present a similar lineshape: a single, roughly symmetric signal at a *g* value of ~2.0035 (see Table 3), typical of carbon-centered radicals derived from the DHICA polymerization process, in agreement with the literature.[45,46] However, a deeper analysis of the spectra of composites shows that the TiO_2-DHICA_ti and TiO_2-DHICA_polym spectra are evidently broader than the DHICA-melanin one. The difference in lineshapes was corroborated by the quantitative determination of the signal amplitude (ΔB). This parameter, detectable by the experimental spectra (see Fig. 3), is related to the mean distance between the radical centers. The ΔB values determined from TiO_2-DHICA_ti and TiO_2-DHICA_polym spectra are similar and significantly lower than the value obtained from the spectrum of DHICA-melanin (Table 3). This evidence indicates that in the hybrid nanoparticles, the radical centers are nearest in their spatial distribution within the nanostructures, probably due to the presence of TiO_2 which modulates the macromolecular organization.

	TiO_2-DHICA_ti	**TiO_2-DHICA_polym**	**DHICA-melanin**
g-factor	2.0034±0.0004	2.0033±0.0004	2.0035±0.0004
ΔB(G)	4.9 ±0.2	5.0 ± 0.2	5.6 ± 0.2
Spin × g^{-1}	5.2×10^{21}	5.1×10^{22}	4.3×10^{23}

Table 3 EPR spectral parameters for hybrid TiO_2-DHICA nanosystems.

To ascertain physical reasons for this experimental evidence, the EPR spectra of the same samples were acquired setting a higher microwave power. An inspection of the normalized power saturation profiles, reported in Fig. 4, shows that, as the microwave power is increased, the spin density increases.

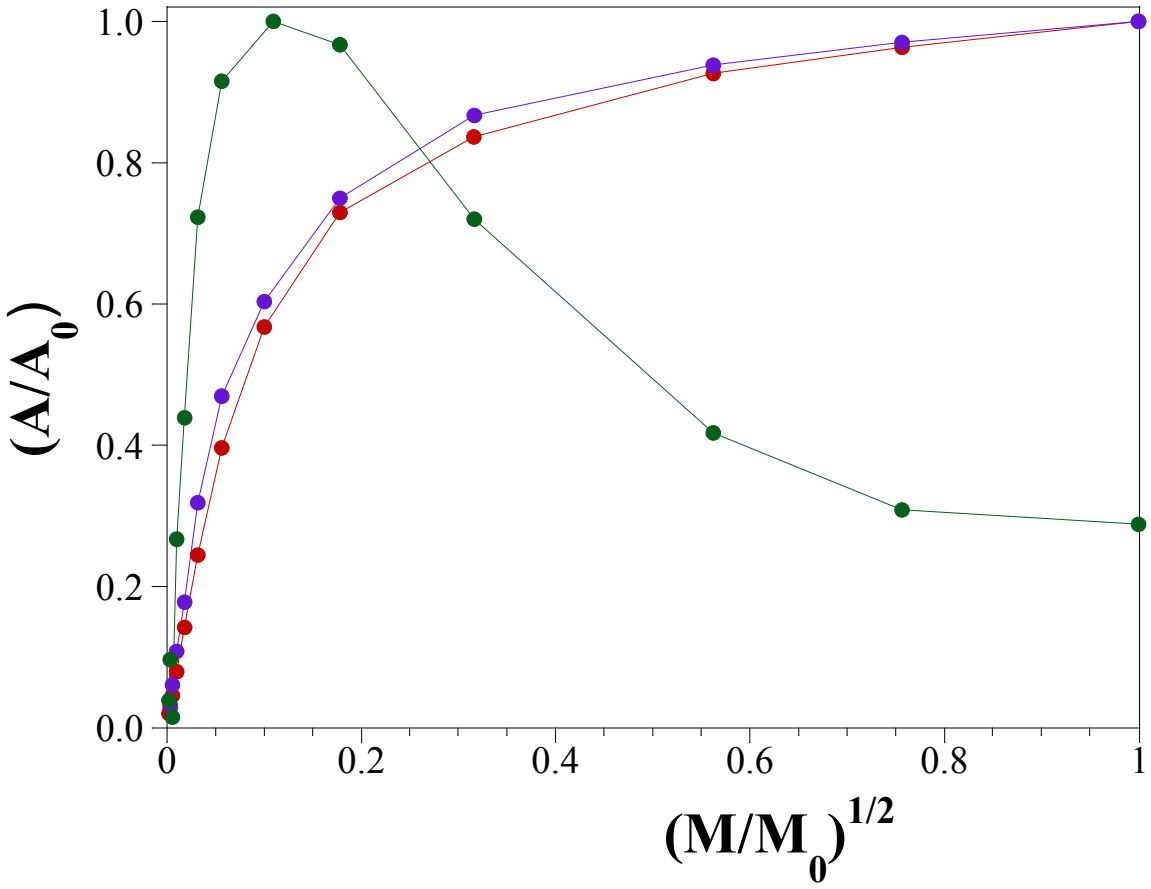

Fig.4 Plot of normalised amplitude vs. power intensities of free radicals of TiO_2-DHICA_ti (red circles), TiO_2-DHICA_polym (purple circles) and DHICA-melanin (greencircles) nanosystems.

Also, the power saturation curves of TiO_2-DHICA_ti and TiO_2-DHICA_polym go to a plateau, in contrast to that observed in the case of DHICA-melanin. Despite very similar *g* values, the quantitative determination of the signal amplitudeΔB and the power saturation profiles suggest a different spatial distribution of the radical centers in the supramolecular organization of the hybrid TiO_2-DHICA_ti and TiO_2-DHICA_polymsystems with respect to the DHICA-melanin. Moreover, the presence of TiO_2 influences the DHICA organization, causing an apparentloss of the typical homogeneous distribution of free-radicals in DHICA melanin[46] associated with a broadening of the signal amplitude in the TiO_2-DHICA_ti and TiO_2-DHICA_polym spectra. It is worth to note, here, that the presence of TiO_2 in DHICA-based samplesproduces power saturation profiles very similar

to that obtained for the pure DHI melanin[46] suggesting an increase in the variety of the radical species in the hybrid nanostructures with respect to the bareDHICA-melanin.

Finally, the quantitative analysis of the spectra intensities demonstrates that TiO_2-DHICA_polym system presents a higher spin density than TiO_2-DHICA_ti (see Table 3).

Diffuse Reflectance UV−VISanalysis

For UV-Vis spectra, the measured intensity was expressed as the value of the Kubelka-Munk function F(R). The energy gap values were calculated by linearization of the plot of $(F(R)h\nu)^{1/2}$ against hν, as reported in Fig. ESI2. For the bare TiO_2, the evaluated optical band gap is 3.2 eV for the transition from the valence band (VB) to conduction band (CB), as well reported in literature.[47] At the same time, the hybrid DHICA-based nanosytems show a decrease in the TiO_2 band-gap of 0.5 eV. Yet, a decrease of intensity of absorption band of TiO_2 within 200 and 400 nm can be appreciated in hybrid systems. This must be due to a shielding effect of melanin towards TiO_2.

Antimicrobial assay

Antimicrobial activity of TiO_2, DHICA and their hybrid nanostructures was tested against *Escherichia coli* DH5α. A concentration of 200 μg/mL of nanoparticles suspension was added to the bacterial cell cultures. Bare $TiO_2$was not very active against the indicator strain**,** as already previously reported,[48] while DHICA-melanin showed a significant amount of activity, leaving the 30% of bacterial cells alive. This result is in agreement with the described function of melanin as part of the innate immune defense system.[18] The combination of TiO_2 and DHICA in the hybrid nanosystems has also been investigated. In the case of TiO_2-DHICA_ti nanoparticles, no antibacterial activity was detected, instead TiO_2-DHICA_polym nanoparticles have shown an excellent antibacterial activity, leaving only the 10% of bacterial cells alive, as observable in Fig. 5. This result can beascribable to the higher radicals concentration in TiO_2-DHICA_polym than TiO_2-DHICA_ti, as determined by EPR, according to the hypothesis of an antimicrobial mechanism

based on the free radical–induced membrane damage.[49-51] Indeed, TiO_2-DHICA_polym shows an higher biocide activity than bare DHICA-melanin, even with a lower radical concentration. This must be due to a broader free-radical species distribution within TiO_2-DHICA_polym, as evidenced by EPR results. This peculiar distribution might improve interaction of these radicals with cells wall, resulting in enhanced antimicrobial activity. Furthermore, higher surface area (Table 2) of TiO_2-DHICA_polym nanostructures may also account for its higher biocide efficacy.

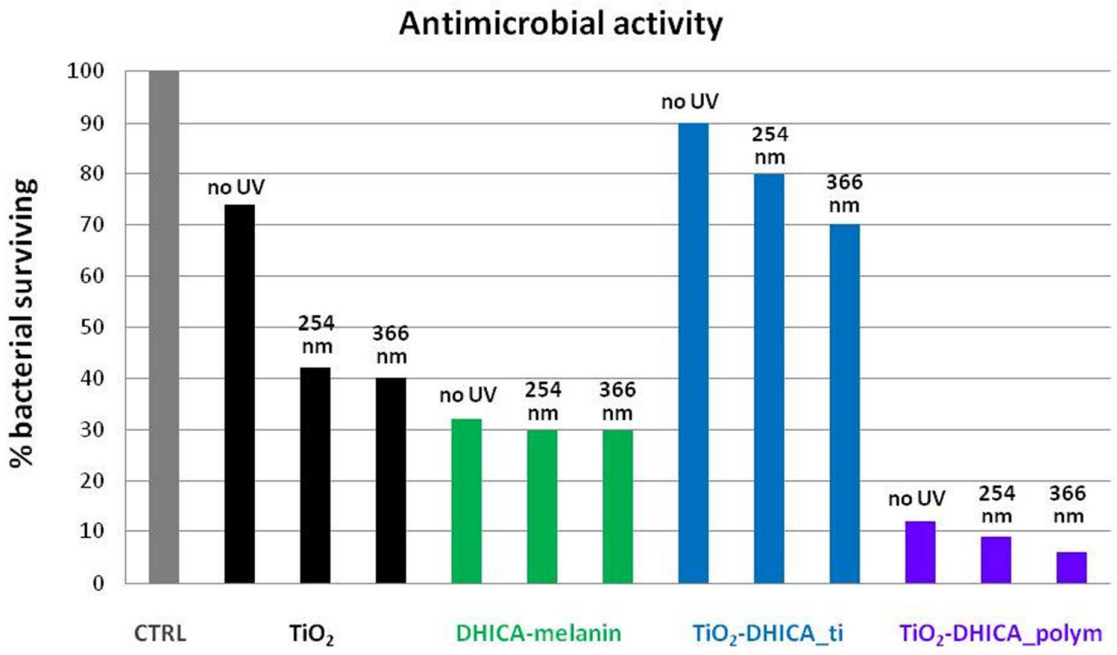

Fig. 5 Antibacterial activity of the different TiO_2-based nanoparticles against *Escherichia coli* DH5α strain. On y-axis is represented the % of bacterial surviving. CTRL bar corresponds to untreated bacterial cells. The other bars represent bacterial survival after treatment with nano-particles containing TiO_2, DHICA-melanin, TiO_2-DHICA_ti and TiO_2-DHICA_polym without irradiation (first bar of each set), with UV irradiation at 254 nm (second bar of each set) and UV irradiation at 366 nm (third bar of each set). The standard deviation was always lower than 5%. Values are reported as means±SEM of three different experiments. $P< 0.05$ (one-way ANOVA followed by Tukey post-test).

The same antibacterial tests were also performed by using all the considered nanoparticles after an UV-irradiation at both 254 and 366 nm. A significant increase of antibacterial activity was observed

overall for bare TiO_2 nanoparticles, as already reported in literature where TiO_2 biocide activity under UV irradiation has been widely assessed.[52,53] On the other hand, the variations in the antimicrobial activity of the other nanosystems were mainly in the range of the standard deviations (see Fig. 4). These results clearly evidence that, with this melanin content (20% w/w), TiO_2 is no longer active as antimicrobial agent even under UV irradiation. This could be ascribed to a UV-shielding effect of DHICAmelanin towards TiO_2,[54] as confirmed by DRUV results.

Conclusion

In the present work, we demonstrated that TiO_2 can catalyze the formation of eumelanin biopolymer from DHICA, leading to the formation of hybrid nanostructures with an eumelanin content of about 20% w/w. These nanomaterials show higher antimicrobial activity towards *Escherichia Coli* bacteria cultures than DHICA-melanin itself, even under visible light. This property must be strictly related to the physico-chemical properties of the investigated systems. In particular, we observed that the DHICA presence during the hydrothermal treatment strongly affects the nanoparticles morphology. All hybrid nanostructures keep the typical anatase crystalline structure and show a mesoporous character, with a higher surface area than DHICA-melanin. Indeed, the presence of TiO_2 influences the DHICA supramolecular organization inducing the generation of a free-radicals variety with respect to the bare DHICA-melanin. This might be associated with a more effective interaction of the available different radical species with cell targets, resulting in an improved antimicrobial activity.

The proposed methodology settles a new role for the inorganic phase, as an active agent in promoting formation of hybrid nanosystems and driving structure of the organic component, opening new perspectives in the design of multifunctional materials.

References

1 G. Kickelbick, in: G. Kickelbick (Ed.), Hybrid Materials, Wiley-VCH, Weinheim, 2007, **1**.

2 C.Sanchez, B. Julian, P. Belleville, M. Popall, *J. Mater. Chem.*, 2005, **15**, 3559-3592.

3 C. Sanchez, P.Belleville, M.Popall, L. Nicole, *Chem. Soc. Rev.*, 2011, **40**, 696-753.

4 G. Prota, Melanins and Melanogenesis; Academic Press: San Diego,CA, 1992.

5 J. J. Nordlund, R. E. Boissy, V. J. Hearing, R. A. King, W. S. Oetting, J. P. Ortonne, Eds.; Blackwell Publishing: Malden, MA, 2.

6 J. D. Nosanchuk, A. L. Rosas, A. Casadevall, *J. Immunol.*,1998, **160**, 6026-6031.

7 N. Avramidis, A. Kourounakis, L. Hadjipetrou, V. Senchuk, *Arzneim Forsch./Drug Res.*,1998,**48**, 764-771.

8 P. Meredith, J. Riesz, *Photochem. Photobiol.*, 2004, **79**, 211-216.

9 S. P. Nighswander-Rempel, J. Riesz, J. Gilmore, J. P. Bothma, P. Meredith, *J. Phys. Chem. B*, 2005, **109**, 20629-20635.

10 S. P. Nighswander-Rempel, *Biopolymers*, 2006, **82**, 631-637.

11 J. B. Nofsinger, T. Ye, J. D. Simon, *J. Phys. Chem. B*, 2001, **105**, 2864-2866.

12 J. Riesz, T. Sarna, P. Meredith, *J. Phys. Chem. B*, 2006, **110**, 13985-13990.

13 T. Ye, J. D. Simon,*J. Phys. Chem. B*, 2003, **107**, 11240-11244.

14 A. Corani, A. Huijser, T. Gustavsson, D. Markovitsi, P. A. Malmqvist, A. Pezzella, M. D'Ischia, V. Sundström, *J. Am. Chem. Soc.*, 2014, **136**, 11626-11635.

15 A. Huijser, A. Pezzella, V. Sundström, *Phys. Chem. Chem. Phys.*, 2011, **13**, 9119-9127.

16 B. J. Bloomfield, M. Alexander, *J. Bacteriol*., 1964, **93**, 1276-1280.

17 M. J. Kuo, M. Alexander, *J. Bacteriol.*,1967,**94**, 624-629.

18 J. A. Mackintosh, *J. Theor. Biol.*,2001, **211**, 101-113.

19 P.Zhao, J. Li, Y. Wang, H. Jiang, *Insect Biochem. Mol. Biol.*2007, **37**, 952-959.

20 M.D'Ischia, K. Wakamatsu, A. Napolitano, S. Briganti, J. C. Garcia-Borron, D. Kovacs, P. Meredith, A. Pezzella, M. Picardo, T. Sarna, J. D. I. Simon, *Pigm. Cell Melanoma Res.* 2013, **26**, 616-633.

21 A. Pezzella, D. Vogna, G. Prota, *Tetrahedron*,2002, **58**, 3681-3687.

22 M. Alfè, D. Spasiano, V. Gargiulo, G. Vitiello, R. Di Capua, R. Marotta, *Appl. Catal. A*, 2014, **487**, 91-99.

23 S. Satyro, R. Marotta, L.Clarizia,I. Di Somma, G. Vitiello, M. Dezotti, G Pinto, R. F. Danats, R. Andreozzi, *Chem. Engin. J.*2014, **251**, 257-268.

24 G. Malloci, M. Binda, A. Petrozza, A. Mattoni, *J. Phys. Chem. C*, 2013, **117**, 13894-13901.

25 R. Edge, *Pigm. Cell. Res.*, 2006, **19**, 443-450.

26 B. Jiang, H. Yin, T. Jiang, *Mater. Chem. Phys.*, 2006, **98**, 231-235.

27 A. Pezzella, L.Capelli, A. Costantini, G. Luciani, F. Tescione, B. Silvestri, G. Vitiello, F. Branda, *Mater. Sci. Engin. C*, 2013, **33**, 347-355.

28 G.Oskam, A. Nellore, R. Lee Penn, P. C. Searson, *J. Phys. Chem. B*, 2003, **107**, 1734-1738.

29 A. Pezzella, M. Barra, M. Musto, A.Navarra, M. Alfè, P. Manini, S. Parisi, A. Cassinese, V. Criscuolo, M. d'Ischia, *Mater. Horiz.*, 2015, DOI: 10.1039/C4MH00097H.

30 A. Napolitano, A. Pezzella, *Tetrahedron*,1996, **52**, 8775-8780.

31 E. P. Barret, L. G. Joynet, P. P. aHalenda, *J. Am. Chem. Soc.*, 1951, **73**, 373-380.

32 N. D.Yordanov, V. Gancheva, V. A. Pelova, *J. Radioanalyt. Nucl. Chem.,* 1999, **240**, 619-622.

33 T. M. Stawski, S. A. Veldhuis, R. Besselink, H. L. Castricum, G. Portale, D. H. A. Blank, J. E. Elshof, *J. Phys. Chem. C*, 2012, **116**, 425–434.

34 T. Lana-Villarreal, A. Rodes, J. M. Pérez, R. Gómez, *J. Am. Chem. Soc.*, 2005, **127**, 12601-12611.

35 S. Varaganti, G. Ramakrishna, *J. Phys. Chem. C*, 2010, **114**, 13917-13925.

36 D.C. Grauer, A. P. Alivisatos, Langmuir, 2014, **30**, 2325−2328.

37 A. Napolitano, M. G. Corradini, G.Prota, *Tetrahedron Letters* 1985, **26**, 2805-2808.

38 G. M. Martin, E. P. Beneditt, N. Eriksen, *Nature,* 1960, **186**, 884-885.

39 H. Zhu, K. Yao, Y. Wo, N. Wang, L. Wang, *Semicond. Sci. Technol*., 2004, **19**, 1020-1023.

40 JCPDS, International Centre for Diffraction Data1998.

41 H.Zhang, M. Finnegan, J. F. Banfield, *Nano Lett*.,2001, **1**, 81-85.

42 J. Sing, K. S. W. Everett, D. H. Haul, R. A. W. Moscou, L. Pierotti, R. A. Rouquerol, J. T. Siemieniewska, *Pure and Appl.Chem.* 1985, **57**, 603-619.

43 E. Cesareo, L.Korkina, G. D'Errico, G. Vitiello, M. S. Aguzzi, F. Passarelli, J. Z. Pedersen, A. Facchiano, *Plos One, 2*012, **7**, e48849.

44 N. F. Della Vecchia, A.Luchini, A. Napolitano, G. D'Errico, G. Vitiello, N. Szekely, M. D'Ischia, L. Paduano, L.*Langmuir*, 2014, **30**, 9811-9818.

45 F.Zuo, L. Wang, T. Wu, Z. Zhang, D. Borchardt, P. Feng, *J. Am. Chem. Soc.,* 2010, **132**, 11856-11857.

46 L. Panzella, L.; Gentile, G.; D'Errico, G.; Della Vecchia, N. F.; Errico, M. E.; Napolitano, A.; Carfagna, C.; d'Ischia, M. *Angew. Chem. Int. Ed*. 2013, **52**, 12684-12687.

47 K. M. Reddy, S. V. Manorama, A. R. Reddy, *Mater. Chem. Phys*., 2002, **78**, 239-245.

48 R. Ahmad, M.Sardar, *Int. J. Inn. Res. in Sci., Eng. Tech*., 2013, **2**, 3569-3574.

49 M. A. Kohanski, D. J. Dwyer, B. Hayete, C. A. Lawrence, J. J. Collins, J. *Cell.,* 2007, **130**, 797-810.

50 J. S. Sung Kim, E. Kuk, K. N. Yu, J. H. Kim, S. J.Park,H. J. Lee, S. H. Kim,Y. K.Park, Y. H.Park,C. Y. Hwang, Y. K.Kim, Y. S.Lee,D. H. Jeong, M. H.Cho, *Nanomed.: Nanotech., Biol. Med.*, 2007, **3**, 95-101.

51 M. A. Kohanski, M. A.DePristo,J. J. Collins,*Molecular Cell.*, 2010, **37**, 311-320.

52 A.Kubacka, M. Ferrer, M. Fernández-García, C. Serrano, M. L. Cerrada, M. Fernández-García, *Appl. Catal. B*, 2011, **104**, 346-352.

53 L. Korösi, D. Dömötör, S.Beke, M. Prato, A. Scarpellini, K. Meczker, G. Schneider, T. Kovács, A. Kovács, S. Papp, *Sci. Adv. Mat*., 2013, **5**, 1184-1192.

54 M. D'Ischia, O. Crescenzi, A. Pezzella, M. Arzillo, L. Panzella, A. Napolitano, V. Barone, *Photochem. Photobiol.* 2008, **84**, 600-607.

Graphical Abstract